

## Structural Characterization and Quantification of Ricinoleic Acid Estolide by NMR Formed During Castor Oil Biodiesel Production

Luiz Silvino Chinelatto Júnior\*, Sonia M. C. Menezes, Fabio L. Farias

PETROBRAS/CENPES/QM, Rio de Janeiro, Brazil

lsilvino@petrobras.com.br

Thiago A. Damasceno

Pontifícia Universidade Católica do Rio de Janeiro (PUC/RJ), Rio de Janeiro, Brazil

Eduardo M. B. Silva

Instituto de Macromoléculas, Centro de Tecnologia, BI J, UFRJ, Rio de Janeiro, Brazil

**Keywords:** *castor bean oil, biodiesel; estolide; <sup>13</sup>C quantitative NMR.*

**Abstract:** *Biodiesel is attracting world attention as an alternative non-toxic, biodegradable and renewable fuel. In this sense, Petrobras has been studying a potential non-edible feedstock for biodiesel production. In this work we describe the study of three biodiesel samples, containing 100, 70 or 30% w/w of castor oil biodiesel, produced in the pilot plant scale. The aim of this work was to develop an analytical method based on NMR for identifying and quantifying all the methanolysis products of castor oil biodiesel. The NMR spectra showed that ricinoleic acid estolide can be formed even in biodiesel samples containing relative small amounts of castor oil (30% w/w). Quantitative <sup>13</sup>C NMR has proved to be a suitable analytical method to monitor all the methanolysis products of castor oil during biodiesel production in the pilot plant scale.*

### Introduction

In order to meet the Brazilian governmental regulations and increase of public awareness to diminish gas emissions, Petrobras has been studying environmental friendly fuels. In this sense, biodiesel is attracting world attention as an alternative, biodegradable and renewable fuel.

Since castor oil is biodegradable and renewable, and non-edible, it is considered an interesting raw material for biodiesel production. Castor oil consists of 89% of 12-hydroxy-9-octadecenoic acid (ricinoleic acid). Other present fatty acids are: linoleic (4.2%), oleic (3.0%), stearic (1.0%), palmitic (1.0%), dihydroxy-stearic (0.5%), linolenic (0.4%) and eicosanoic (0.4%). The chemistry of castor oil is centered on its high content of ricinoleic acid

and the three points of functionality existing in this molecule, making it suitable for many chemical reactions and modifications. These are: (1) the carboxyl group which can be a point of esterification; (2) the single point of unsaturation in carbon 9 which can be altered by hydrogenation, epoxidation or vulcanization; and (3) the hydroxyl group in carbon 12 which can be acetylated or alkylated. Due to this wide range of chemical possibilities, the analysis of the reaction products of this feedstock is not straightforward. For this reason, the recommended chromatographic method described in the standard method NBR 15342 can not be applied to intermediates fractions of the castor oil transesterification reaction.<sup>1</sup>

Supported by the world's interests on biodiesel production, nuclear magnetic

resonance spectroscopy (NMR) is playing an increasing role in the study of oil chemistry during the last years. NMR measurement is also expected to provide detailed insights into pathways of the transesterification reaction of oils. Gelbard *et al.*<sup>2</sup> first reported that the yield of transesterification reaction can be determined by <sup>1</sup>H NMR analysis.

In this study, we report an analytical method based on NMR to identify and quantify all methanolysis products from castor oil.

## Experimental

### *Biodiesel samples*

The castor oil and mixture of castor oil and soybean biodiesel used in this work were produced by transesterification of commercial castor and soybean oils with methanol using a homogeneous alkaline catalyst in a biodiesel pilot plant installed in the Petrobras Research and Development Center in Rio de Janeiro – Brazil. In this work three different intermediate samples were used: 1) castor oil biodiesel; 2) castor oil (30%) soybean (70%) w/w biodiesel and 3) castor oil (70%) soybean (30%) w/w biodiesel. These three samples were collected in the same specific step of the industrial process (after the second reactor).

### *NMR analysis*

<sup>1</sup>H, <sup>13</sup>C, gCOSY and gHMBC experiments were performed on a Varian 400MR equipment (9.40 T of magnetic field) at room temperature (27 °C) and the samples were dissolved in CDCl<sub>3</sub> containing 0.05% v/v TMS used as internal reference (0 ppm). The <sup>13</sup>C quantitative NMR experiments were recorded in a 10 mm probe and all others in a 5 mm probe. The <sup>1</sup>H NMR spectra of 5% v/v solutions were acquired with the observation frequency of

399.8 MHz, using 45° rf pulses, relaxation delay of 1.0 s, acquisition time of 2.05 s, spectral width of 6410.3 Hz and 128 transients were accumulated. The <sup>1</sup>H NMR spectra were processed using a line of 0.3 Hz. The <sup>13</sup>C NMR spectra of 40% v/v solutions were acquired with the observation frequency of 100.5 MHz, using 90° rf pulses, relaxation delay of 10 s, acquisition time of 1.3 s, spectral width of 24509.8 Hz and 1024 transients were accumulated. The decoupler was set in the gated mode to avoid NOE. The <sup>13</sup>C spectra were processed using a line of 1.0 Hz. The gCOSY spectra of 10% v/v solutions were acquired with 256 F1 increments, 8 transients per increment, relaxation delay of 1.0 s, acquisition time of 0.167 s and recorded with 2048 x 2048 data points. A weighting function was applied to each dimension and zero filled to 2 K points. For the gHMBC spectra of 10% v/v solutions, the long-range coupling constant of 8.0 Hz was used to set delays in the pulse sequence. They were acquired with 400 F1 increments, 32 transients per increment, relaxation delay of 1.0 s, acquisition time of 0.128 s, recorded with 4096 x 4096 data points and with a <sup>1</sup>H-<sup>13</sup>C *J*-evolution delay of 80 ms. A sine bell processing was applied to both <sup>1</sup>H and <sup>13</sup>C dimensions and zero filled to 4 K and 1 K points, respectively. The HMQC spectra of 10% v/v CDCl<sub>3</sub> (0.05% v/v TMS) solutions were obtained on a Varian Mercury 300 (7.05 T of magnetic field), at room temperature (27 °C). The one-bond coupling constant of 140.0 Hz was used to set delays in the pulse sequence and spectra were recorded using 2x160 F1 increments, 32 transients per increment, relaxation delay of 1.0 s, acquisition time of 0.170 s and filling with 1024 x 2048 data points. A sine bell processing was applied to

both F1 and F2 dimensions before zero filling to both F1 and 2 K points and Fourier transformation.

### Results and Discussion

The detailed pathways of the transesterification of castor oil are not well-known yet. Most research on this feedstock was only based on the traditional stepwise reaction of: triglycerides (**TGs**)  $\rightarrow$  *sn*-diglycerides (**DGs**) + esters (**ES**)  $\rightarrow$  *sn*-monoglycerides (**MGs**) + **ES**  $\rightarrow$  glycerol (**G**) + **ES**, without considering other side reaction possibly because of the lack of appropriate analytical methods.

During Petrobras research on castor oil biodiesel production in the pilot plant scale, it was observed that the levels of diglycerides were typically higher in these samples than in biodiesel from other vegetable oils or animal fats. This fact was always attributed to the difficulty of castor oil biodiesel to meet specifications and because of its non-traditional chromatographic profile, rather than

the formation of unusual side compounds during the transesterification reaction. The NMR analysis of a sample in which the chromatogram consisted in a group of overlapping peaks in the diglycerides region, proved the formation of ricinoleic acid estolide shown in Figure 1, under base-catalyzed conditions.

An estolide is an oligomeric fatty acid (or ester) which contains secondary ester linkages on the alkyl backbone of the molecule.<sup>3,4</sup> Estolides have been found in nature,<sup>5</sup> and have been synthesized in laboratory.<sup>3,4</sup>

There are two mechanistic pathways for the formation of estolides: (1) condensation of the hydroxyl functionality of the hydroxyl fatty acid with the carboxylic acid function of another fatty acid (or ester) forming the compound shown in Figure 1 and (2) the carbocationic homo-oligomerization of unsaturated fatty acids resulting in the addition of a fatty acid carboxyl to the olefinic carbon forming the compound shown in Figure 2.

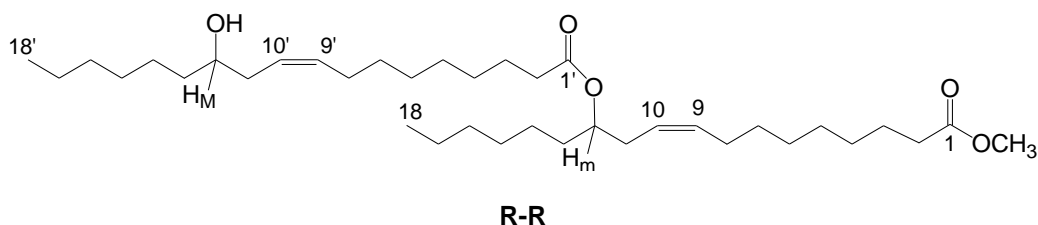


**Figure 1.** Structure of ricinoleic acid estolide formed during castor oil biodiesel production under base-catalyzed conditions. R-R means: ricinoleic – ricinoleic dimer.

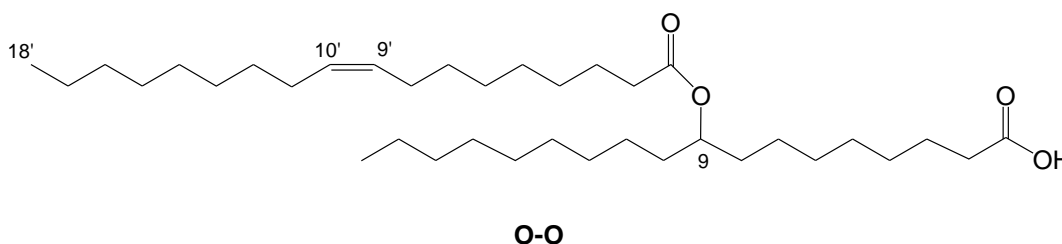


**Figure 2.** Structure of oleic acid estolide synthesized in laboratory through carbocationic homo-oligomerization of unsaturated fatty acids.<sup>4</sup> O-O means: oleic – oleic dimer.

A key feature of the  $^1\text{H}$  NMR spectra of the castor oil biodiesel samples studied is the estolide methine proton signal ( $\text{H}_m$  in Figure 1) at 4.9 ppm. The  $\text{H}_m$  proton signal arises apart from the hydroxyl methine resonance at 3.6 ppm ( $\text{H}_M$ ), and has a multiplet coupling pattern as expected for a proton between two non-equivalent methylenes. The main feature of the  $^{13}\text{C}$  NMR spectra of the castor oil biodiesel samples studied is the estolide methine carbon signal  $\text{C}_m$  (see the carbon directly bonded to  $\text{H}_m$  proton in Figure 1) at 73.6 ppm which increases simultaneously with the decreasing intensity of the  $\text{C}12'$  hydroxyl carbon peak at 71.3 ppm. The  $\text{C}_m$  assignment was confirmed by the HMQC experiment (see Table 1). Other key spectral features are: (1) the appearance of the oleate-olefinic carbons at  $\delta 131.4\text{ppm}$  and  $\delta 124.0\text{ppm}$  and (2) the appearance of the estolide carbonyl carbon at 173.2ppm.

The gHMBC spectrum shown in Figure 3 shows that the methine  $\text{H}_m$  proton signal at 4.9 ppm is correlated to the carbonyl signal at 173.2 ppm and to the olefinic carbon signal at 131.4 ppm, supporting the presence of the estolide.

In order to investigate the oligomer length of the estolide present in the castor oil biodiesel samples studied, a Gel Permeation Chromatography experiment was performed (data not shown). This experiment indicated the existence of a monodisperse dimer (a monoestolide), supporting the formation of the ricinoleic acid estolide shown in Figure 1.

An explanation for the termination of the oligomerization with the formation of dimers, is that there is no apparent reason for the esterification to occur exclusively by condensation of two ricinoleic fatty acids.

**Table 1.** HMQC NMR data for the castor oil biodiesel sample studied

Functional group	$\delta\text{C}$ (ppm)	$\delta\text{H}$ (ppm)
<b>C=O</b>	173.7; 173.2	-
<b>-CH=CH-</b>	132.1; 131.4 129.6; 129.5; 129.3 127.6; 127.5 125.2; 124.0; 120.0	5.6 – 5.5 5.2 – 5.1 5.2 – 5.1 5.5 – 5.1
<b>C9/H9</b> and <b>C12/H12</b> of dihydroxystearic acid derivatives	74.6	3.5
<b>C<sub>m</sub></b> and <b>H<sub>m</sub></b>	73.6	4.9
<b>C12/H12</b> of ricinoleic acid derivatives (containing hydroxyl group)	71.3	3.6
<b>-OCH<sub>3</sub></b>	50.9	3.6
<b>-CH<sub>2</sub>-CH(OH)-CH<sub>2</sub>-CH<sub>2</sub>-</b> and <b>-CH<sub>2</sub>-CH(OCOOR)-CH<sub>2</sub>-CH<sub>2</sub>-</b>	36.5	1.4
<b>-CH=CH-CH<sub>2</sub>-CH(OH)-</b> and <b>-CH=CH-CH<sub>2</sub>-CH(OCOOR)-</b>	35.0	2.1
<b>-CH<sub>2</sub>COOR</b>	34.2	2.2
<b>-CH<sub>2</sub>-</b>	31.6; 29.4; 29.2; 29.1; 29.0; 28.9; 28.8; 28.7; 28.6	1.1 – 1.3
<b>-CH<sub>2</sub>CH<sub>2</sub>-CH=CH-</b>	27.0	2.1
<b>-CH<sub>2</sub>-CH(OH)-CH<sub>2</sub>CH<sub>2</sub>-</b> and <b>-CH<sub>2</sub>-CH(OCOOR)-CH<sub>2</sub>CH<sub>2</sub>-</b>	25.4	1.3
<b>-CH<sub>2</sub>-CH<sub>2</sub>COOR</b>	24.7	1.6
<b>-CH<sub>2</sub>-</b>	22.3; 22.2	1.1 – 1.3
<b>-CH<sub>3</sub></b>	13.7; 13.5	0.9

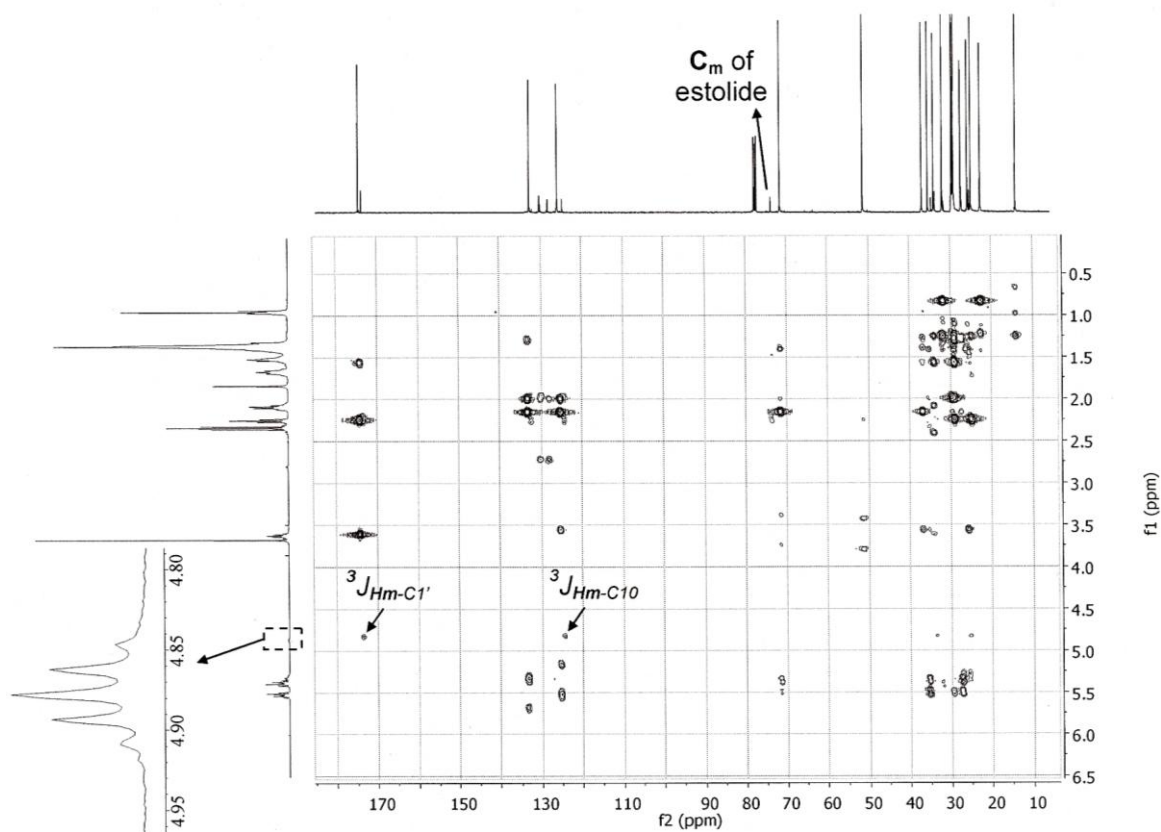


**Figure 3.** gHMBC NMR spectrum of the castor oil biodiesel sample studied. Note two typical  $^3J_{H-C}$  correlations for the methine  $H_m$  proton (4.9 ppm) of estolide.

Owing to the presence of different fatty acids in the reaction medium, like oleic, linoleic, stearic acids, and others, although in much less amount, several classes of monoestolides can be formed. Then a wide range of dimers can be formed by condensing one ricinoleic acid with another fatty acid. Consequently, the estolide is interrupted at this point from further growth. This has a higher probability in biodiesel samples formed from a mixture of castor oil with other vegetable oils or animal fats, as they are composed of many different fatty acids. As an example, in Figure 4 are represented four types of dimers possibly found in a mixture of castor oil and soybean biodiesel samples.

The NMR analysis of a raw castor oil and the corresponding refined castor oil sample (both of them, before transesterification) demonstrate that these samples were free of ricinoleic acid estolide (or ricinoleic triglyceride estolide), proving that the estolide shown in Figure 1 is formed during castor oil transesterification. Indeed, in biodiesel samples produced from other vegetable oils or animal fats (containing no hydroxyl ester derivatives) in the biodiesel pilot plant at Petrobras Research and Development Center, no kind of estolide derivative could be observed. Even those estolide formed from the reaction of a carboxylic acid of one fatty acid with the unsaturation site of another fatty acid, forming an ester linkage, were detected. This

fact proves that the hydroxyl group plays an important role in the estolide formation during the biodiesel production from castor oil or its blends.

As biodiesel must be comprised of 96.5% w/w minimum of mono-alkyl esters of long chain fatty acids derived from vegetable oils or animal fats, one question emerging from the existence of a dimer of ricinoleic acid in the castor oil biodiesel, is the fact that this compound will prevent the fuel to meet specifications. It is then necessary to monitor

this biodiesel by some analytical method. As mentioned before, in the intermediate fractions of the transesterification reaction, containing high levels of acylglycerols and methanol, the chromatographic method described in the standard method NBR 15342 can not be applied because of the existence of the overlapping peaks in the chromatogram (data not shown) as well as the ineffectiveness of the derivatization process with N-methyl-N-trimethylsilyltrifluoroacetamide (as described in the standard method ASTM D6584).

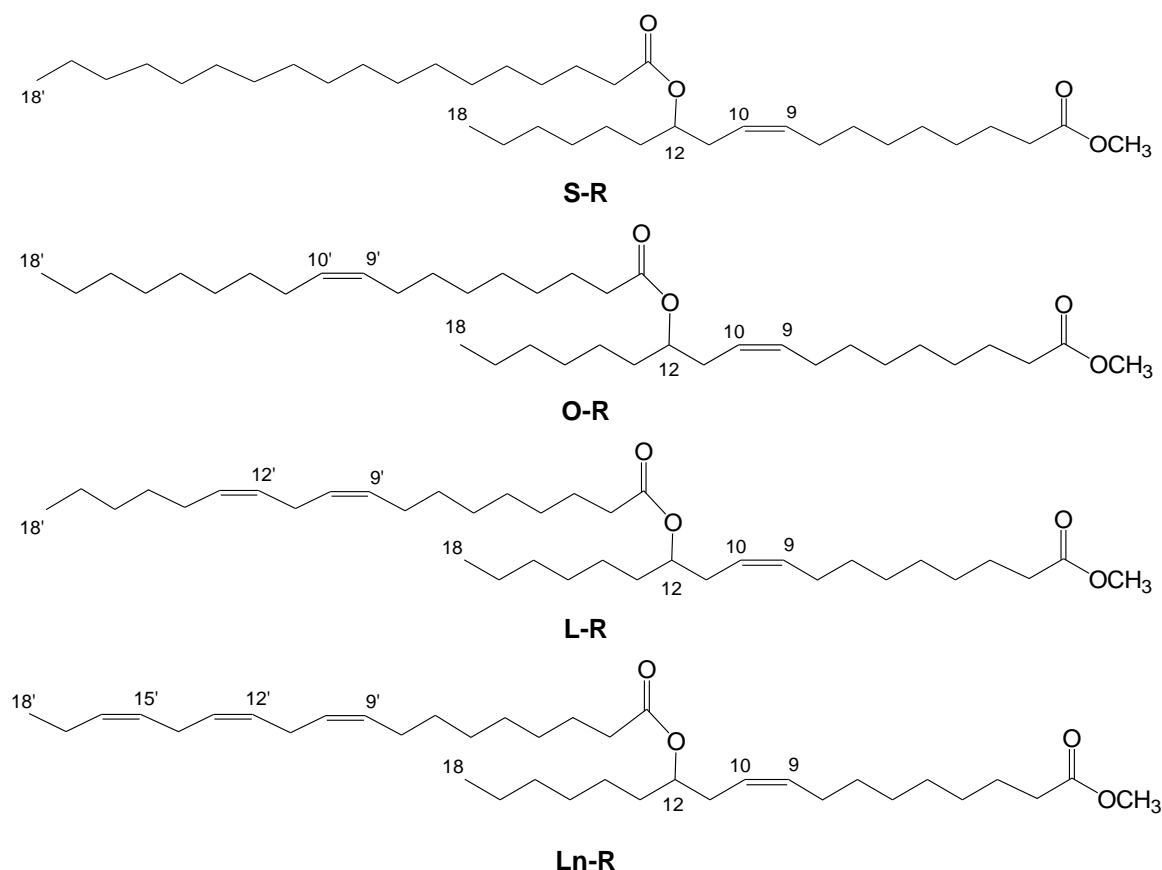


**Figure 4.** Structure of four different monoestolides possibly found in a mixture of castor and soybean biodiesel samples. S, O, L, Ln and R means: stearic, oleic, linoleic, linolenic and ricinoleic acid, respectively.

As the signal of  $H_m$  proton at 4.9 ppm can be overlapped by the H-2 glycerol proton of the *sn*-2-monoglyceride (2-MG), when this monoglyceride is present in the biodiesel sample (see Figure 5), the suitable way to quantify the dimer of ricinoleic acid is by using  $^{13}C$  NMR in quantitative experimental conditions. In this sense, the quantitative  $^{13}C$  NMR spectrum was obtained using gated

proton-decoupling mode in order to suppress the nuclear *Overhauser* effect (NOE), and a relaxation delay at least 5 times the longest spin-lattice relaxation time,  $T_1$ .<sup>6</sup>

According to the literature, the  $T_1$  values of the carbons corresponding to the methanolysis products of biodiesel samples in the region between 74.0 and 49.5 ppm range from 0.22 to 0.99 s.<sup>7-9</sup>

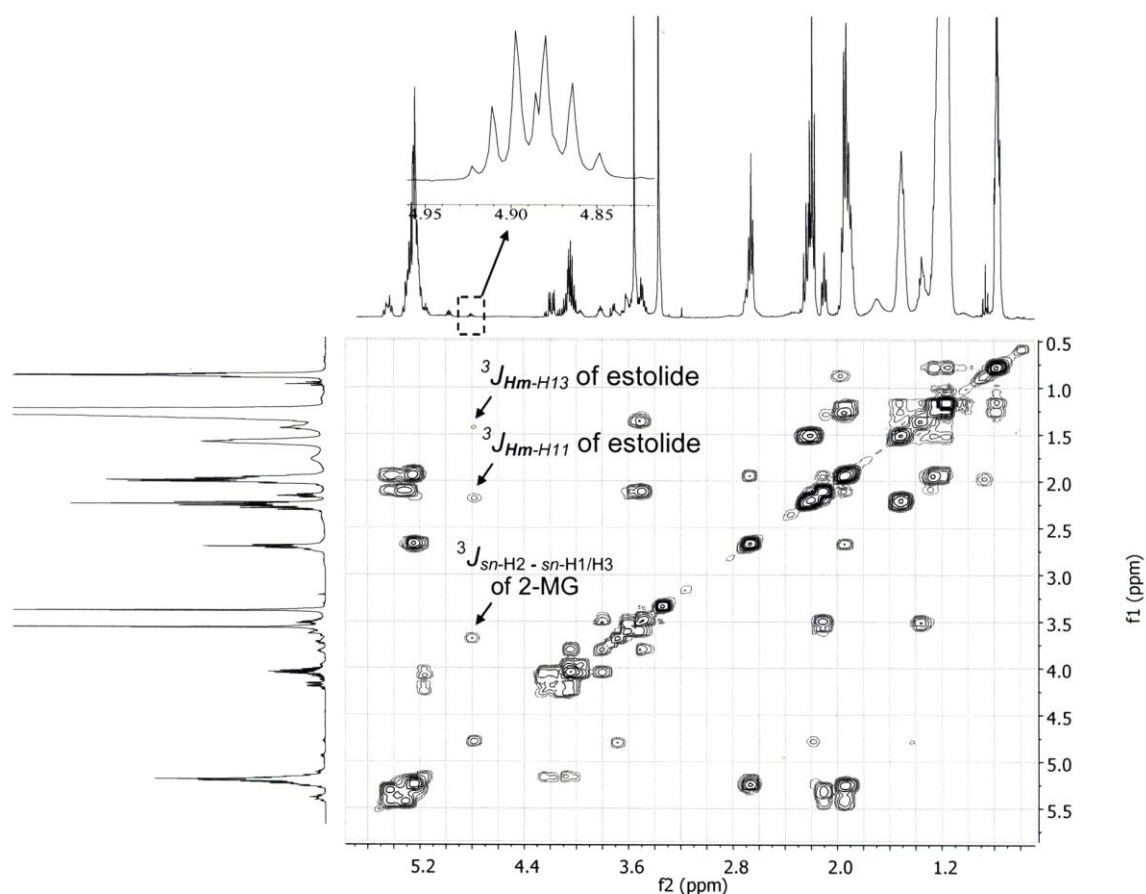


**Figure 5.** gCOSY NMR spectrum of the intermediate castor oil (30%) soybean (70%) w/w biodiesel sample studied. Note the overlapping of the *sn*-H2 proton of 2-MG with the methine  $H_m$  proton of estolide (inset) and the following correlations for these two protons:  $^3J_{Hm-H13}$  of estolide,  $^3J_{Hm-H11}$  of estolide and  $^3J_{sn-H2 - sn-H1/H3}$  of 2-MG.

To determine the dimer of ricinoleic acid (estolide), as well as the others methanolysis products of castor oil biodiesel by  $^{13}\text{C}$  quantitative NMR, it is only necessary to integrate the areas of peaks of spectrum in the region between 74.0 and 49.5 ppm (see Figure 6). The peaks are well separated, except for C-2 glycerol carbon of 2-MG, which overlaps with the peak at 67.6 ppm for the C-2 glycerol carbon of 1,3-DG. The proportion of TG

species in the sample is represented by the total integrated intensity of the peak of the C-2 glycerol carbon at 68.8 ppm. The MG species are easily quantified by the sum of the total integrated intensity of the peak of the C-2 glycerol carbon of the 1-MG at 70.0 ppm, and half of the integrated intensity of the peak of the C-1/C-3 glycerol carbon of the 2-MG at 61.5 ppm.

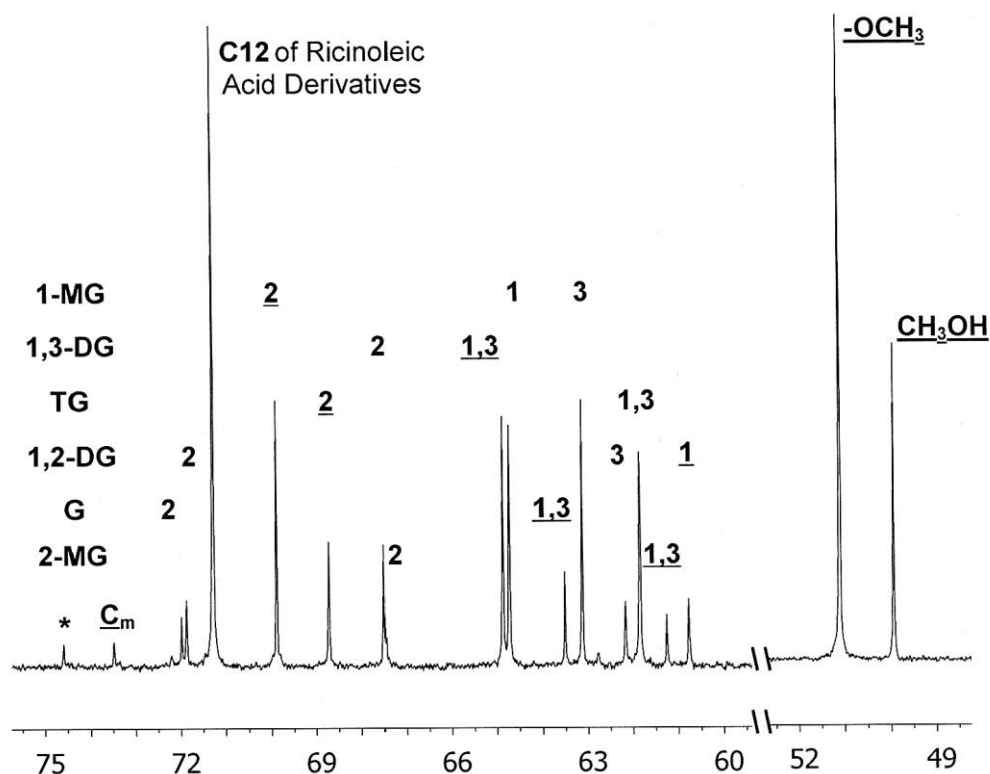


**Figure 6.** Glycerol carbon region (75.7 to 59.5 ppm) and methoxy region (52.7 to 48.2 ppm) of the  $^{13}\text{C}$  NMR spectrum of the intermediate castor oil (70%) soybean (30%) w/w biodiesel sample.  $\text{C}_m$  is the methine carbon of the estolide. Each glycerol carbon (designated as 1, 2, and 3) of each species of acylglycerol is labeled horizontally as: TG = triacylglycerol, DG = diacylglycerol, MG = monoacylglycerol and G = free glycerol, and vertically with the respective glycerol carbon peak position. \* $\text{C}_9$  and  $\text{C}_{12}$  of dihydroxy stearic acid derivatives. The underlined peaks indicated with numbers or letters can be used for quantification.

The DG species are easily quantified by the sum of half of the integrated intensity of the peak of the C-1/C3 glycerol carbon of the 1,3-DG at 65.0 ppm and the total integrated intensity of the peak of the C-3 glycerol carbon of the 1,2-DG at 60.8 ppm. Half of the integrated intensity of the peak for its C-1/C3 carbon at 63.6 ppm represents the mole fraction of free glycerol (G).

The total integrated area of the peak at 73.6 ppm represents the mole fraction of the estolide. Finally, the peaks corresponding to methanol and the methoxy group of methyl esters lie exclusively in the region between 49.5 – 51.5 ppm and the total integrated intensities of these two peaks provide the mole fractions of these species in the biodiesel sample. In order to obtain the proportion of each species directly from the spectrum, without further calculation, total area of the peaks discussed above should be set as 100. Other combinations of peak areas can also be useful for quantification.

According to the Ng S. work,<sup>6</sup> the presence of free fatty acids is easily detected and quantified in the region of the spectrum corresponding to the aliphatic carbons (according to this reference, the C-3 of free fatty acids appears at 24.7 ppm). Due to the fact that the chemical shift data of the glycerol carbons (as well as the methoxy carbons) in biodiesel samples are practically independent of the nature of the fatty acid, the methodology described in this work can be applied to biodiesel samples produced from almost any vegetable oils or animal fats.

## Conclusions

These results lead to the conclusion that the compound shown in Figure 1 is formed under base-catalyzed conditions, during castor oil biodiesel production. The hydroxyl group present in the ricinoleic acid and derivatives plays an important role in the estolide formation during the biodiesel production. The NMR spectra showed that ricinoleic acid estolide can be formed even in biodiesel samples containing relative small amounts of castor oil (30% w/w). Quantitative <sup>13</sup>C NMR has proved to be a suitable analytical method to monitor all the methanolysis products of castor oil during biodiesel production in the pilot plant scale.

## Acknowledgments

The authors would like to acknowledge Flavio Cortinas Albuquerque and Fátima Regina Dutra Faria (Petrobras Research and Development Center) for performing the Gel Permeation Chromatography and the Gas Chromatography experiments, respectively.

## References

1. ABNT - Associação Brasileira de Normas Técnicas  
<http://www.abnt.org.br/default.asp?resolucao=1152X864> (Access in May 2008).
2. Gelbard, G.; Bres, O.; Vargas, R. M.; Vielfaure, F.; Schuchardt, U. F.; *J. Am. Oil Chem. Soc.* **72** (1995) 1239.
3. Isbell, T. A.; Lowery, B. A.; DeKeyser, S. S.; Winchell, M. L.; Cermak, S. C.; *Ind. Crops and Prod.* **23** (2006) 256.
4. Isbell, T. A.; Kleiman, R.; Plattner, B. A.; *J. Am. Oil Chem. Soc.* **71** (1994) 169.

5. Plattner, R. D.; Payne-Wahl, K.; Tjarks, L.; Kleiman, R.; *Lipids*, **14** (1979) 576.
6. R. Harris: Nuclear Magnetic Resonance Spectroscopy, Longman Scientific & Technical, Harlow, Essex (UK) 1986, pp. 107-114.
7. Ng, S. *J. Am. Oil Chem. Soc.* **77** (2000) 749.
8. Vlahov, G. *Prog. Nucl. Magn. Reson. Spectrosc.* **35** (1999) 341.
9. Alemany, L. B. *Chem. Phys. Lipids* **120** (2002) 33.